2005 American Control Conference
June 8-10, 2005. Portland, OR, USA

Experimental Investigation of Disc Drive Seek Control When Subject to a Nonlinear Magnetic Bias

Ryan Ratliff
Mechanical and Aerospace Engineering
Oklahoma State University
Stillwater, OK 74078
ryan.ratliff@okstate.edu

Prabhakar Pagilla
Mechanical and Aerospace Engineering
Oklahoma State University
Stillwater, OK 74078
pagilla@ceat.okstate.edu

Abstract— **The research experimentally investigates the design and performance capabilities of a voice-coil motor actuator (VCMA) for a disc drive with a nonlinear magnetic bias. A magnetic bias feature is independently designed on the actuator arm to compensate for non-operational shock. Because the resulting bias is nonlinear and uncertain, a model-based adaptive controller was developed to meet seek performance requirements and simultaneously handle effects of the nonlinear bias. Although exact characterization of the bias was unknown, bounds could be determined from geometric tolerance analysis. A projection algorithm was implemented to maintain the bias estimate within the known bounds. The performance criteria was based on minimizing the time required for a seek maneuver without controller saturation. Extensive experiments were conducted to characterize the VCMA physical parameters and verify the controller performance. Additionally, efforts were made to investigate the effects of sample rate variation and bias modeling errors. A representative sample of the results is presented and discussed.**

I. INTRODUCTION

The read/write (R/W) heads of a hard disc drive are very sensitive to external shock and vibration. Shock and vibration dynamics can cause head/disc impact. If the impact occurs in the area of the disc where data is stored, data loss or permanent damage can occur. Typically, there is a maximum shock and vibration specification limit that corresponds to a given head design. Shock specifications are given for both operational and non-operational states. Disc drives will typically see higher shock levels during the non-operational state primarily resulting from shipping and handling. Modern designs incorporate latching or locking mechanisms to hold the actuator arm at a specific position when the drive is not in operation. This allows higher non-operational dynamics to be tolerated and prevents a fatal event, caused by a drop or careless handling, that would physically damage the drive. The majority of the latch designs that exist today are passive and require external sources of mechanical energy. For example, certain latch designs take advantage of the high velocity airflow generated by the spinning discs for actuation [1]. Other designs rely on the inertia of a separate member that moves when a shock is imparted to the drive [2]. Although not as common, some latches are designed to take advantage of magnetic forces that are inherent in the magnetic circuit or supplied by a separate magnet [3], [4].

One design [5] presents a low cost, non-contact solution. A ferrous member attached to the actuator arm is attracted to the magnetic field of the VCMA magnetic circuit. In order to resist most shocks, the bias is required to be active for most of the actuator stroke angle. Typically, the bias torque is nonlinear and significant compared to the actuator torque available which can have detrimental effects on seek performance. Geometric tolerances result in a distribution of bias curves when considering a production population of drives. Therefore, the bias enters the system as an unmatched uncertainty which causes additional challenges for seek controller design. Recent research has focused on the effects of a large magnetic bias on seek performance and simulation studies were performed to determine if nonlinear control methods could be proven effective [6]. It was determined that knowing the nominal and bounding characteristic of the magnetic bias, a stable, adaptive controller could be designed to compensate for the bias effects and improve performance.

In this research, a bias feature is designed to restore the actuator arm back to the nominal shipping location after the impact of a rotary shock. A special disc drive is manufactured with the corresponding bias design. A third-order dynamic model for the VCMA with the added bias feature is developed. Bounds on the magnetic bias magnitude and position is determined based on known geometric tolerance studies. A stable, adaptive seek controller is designed based on the dynamic model and experiments are conducted using a laser vibrometer for position and velocity feedback. A projection algorithm is implemented to limit the bias estimate to within the known bounding tolerances. A performance comparison is made on the effects of sample rate and accuracy of nominal bias approximation. Section II discusses common latching mechanisms and the issues associated with each. The dynamic model of the VCMA that includes the nonlinearity due to the arm bias is given in Section III. Section IV contains the development of a model reference adaptive controller that compensates for bias uncertainties. To keep bias estimates within toleranced bounds, a projection algorithm is also discussed. Com-

This work was supported in part by the U.S. National Science Foundation under Grant No. CMS 9982071. The authors would like to thank Seagate Technology for providing resources to help make this work possible.

parative experimental results are discussed in Section V. Conclusions and future research are given in Section VI.

II. LATCH COMPARISON

Air vane and inertial style latches are the most commonly used in industry today. Both styles are preferred for their high shock resistance capabilities. Inertial latches are common in drives sized for notebook computers and consumer electronics. An inertial-style latch is shown in Figure 1. The latch consists of a separate inertial member rotating about a designated pivot point. Both the pivot location and inertia of the member are designed so that the member engages the actuator arm in a finite time under the influence of a specified shock. The engagement contact effectively blocks actuator motion and prevents the R/W heads from moving into the data zone. The timing of this engagement can become problematic, inconsistent, or even impossible if wide ranges of shock resistance are required. For example, the latch design may meet a specified upper amplitude limit at the expense of lower amplitudes. It is possible for inertial latches to engage the actuator at higher shock amplitudes, but "miss" at lower amplitudes.

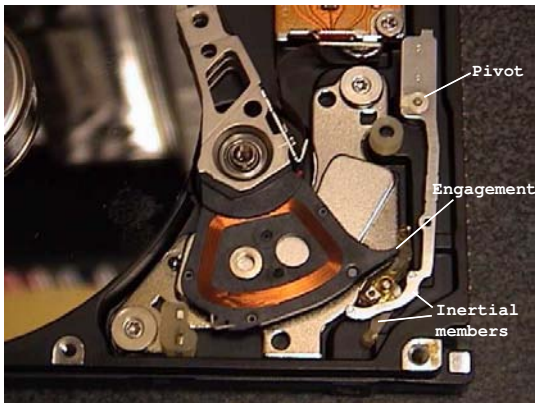

Fig. 1. Inertial latch (Courtesy of Fujitsu Computer Systems Corp).

Air latches are typically found in desktop and server drives where larger disc sizes and higher spindle speeds provide stronger air flow currents. Figure 2 depicts an air latch consisting of a small, nominal, return bias and a "vane" member that protrudes radially along the discs obstructing potential airflow. Opposite the air vane is an engagement feature that keeps the actuator arm locked in shipping position when the drive is off. When power is applied to the drive, force is applied to the latch vane as a result of the airflow from spinning discs. The latch overcomes the return bias and stays open as long as power is applied and the discs are spinning. Disc drive manufacturers typically benefit from reducing the disc count or "depopulating" a given product. This allows the manufacturer to design only one set of mechanics and provide customers with different levels of capacity. Reducing the disc count, however, would obviously change the dynamics of the air latch operation. Therefore, difficulties can arise in implementation of a common air latch with a product scheduled for depopulation. Multiple latch designs may be required which is undesirable.

Magnetic, bi-stable latches are not as common because of their low shock resistance capability. They are typically found in high-end server drives where shock requirements are not so stringent. The bi-stable latch is called such because it has two stable equilibrium points. A typical bi-stable latch is shown in Figure 3. A plastic member rotates about a designated pivot pin. A magnet is molded into the plastic member and is attracted to two separate steel pins. The proximity of the magnet determines to which pin the magnet is attracted. A properly designed bistable latch is not allowed to rest in between the two pins. The engagement contact dynamics between the latch and actuator arm are analogous to that of two spur gears. The latch is actuated by the disc drive actuator itself. Hence, when the is latch closed, it is required to overcome the actuator arm inertia subject to a rotational shock. Conversely, the disc drive actuator must overcome the latch holding force when the drive is powered on. So the latch holding torque requirement conflicts with the actuator arm opening torque requirement. Most bi-stable latches are positioned behind the actuator limiting the coil length. A longer coil generally results in higher torque capability of the actuator. Also, because there is impact involved during latching, the potential exists for particulate generation which can be fatal to a disc drive.

All three of the previously mentioned latches result in additional cost that can become significant in high volume products. The following research focuses on fulfilling the shock resistance requirements using a pure magnetic bias that results in significantly reduced cost and virtually none of the issues mentioned above. A magnetic bias is induced on the actuator by attaching a steel object to the arm that rotates in the magnetic air gap of the VCMA. This latching mechanism has the advantage of a single, inexpensive mechanical part. Additionally, the size of the VCMA is less restricted so motor performance can be optimized. The disadvantage is that the bias force is nonlinear, and exists over most, if not all, of the actuator stroke which influences drive operation and seek controller performance. Further, the bias force nonlinearity is an unmatched uncertainty [7], which presents an additional challenge for the seek controller design. Even if the bounds on the bias are known, the worst case bias value would have to be used as an estimate for all drives in order to prevent saturation. If the bias could be estimated for each individual drive, some seek performance could be obtained on drives that do not represent worst case. A seek controller must be developed that can compensate for uncertain bias nonlinearities without sacrificing performance. Alternatively, it may be desirable to sacrifice some seek performance for a justified cost savings in the latch.

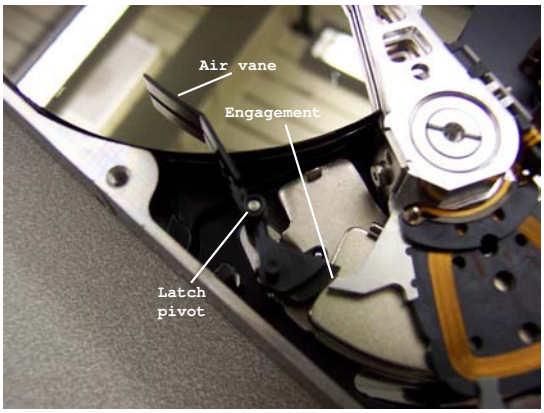

Fig. 2. Air latch concept (Courtesy of Quantum Corp).

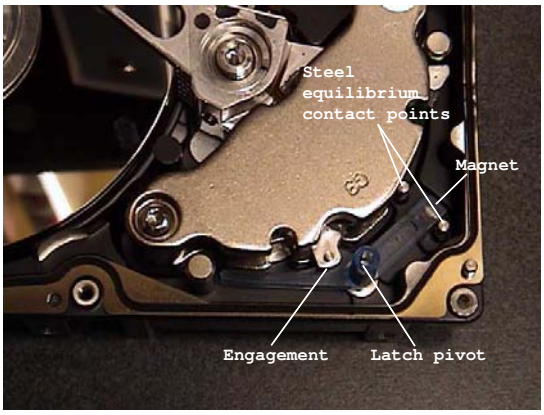

Fig. 3. Bi-stable latch concept (Courtesy of Seagate Technology).

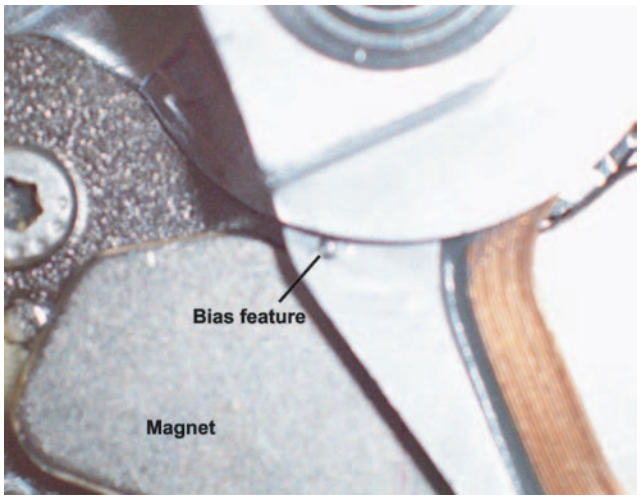

Fig. 4. Magnetic bias concept

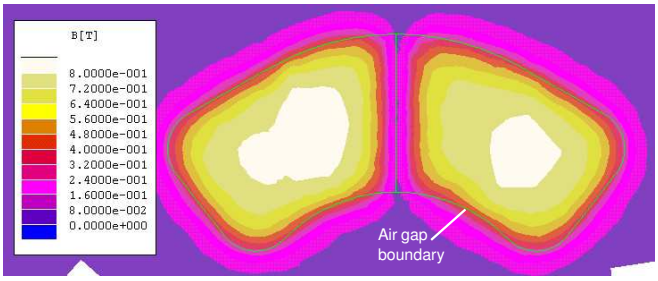

Fig. 5. Air gap flux density

III. MODELING

It was necessary to design a bias across the sweep angle to restore the arm back to the nominal shipping location after the impact of a rotational shock. The strategy was to design a bias torque that applies an energy equivalent to that of the shock, thus bringing the arm to rest after traveling a desired angular displacement. A passive bias was desirable and could be obtained by attaching a steel feature to the actuator arm, partially protruding into the air gap of the magnetic circuit as shown in Figure 4. Ideally, a constant bias torque would be most advantageous for controller design. Unfortunately, this is not the case for the passive bias used. The magnetic flux density in the air gap is most uniform at the center. The flux density gradient increases as the air gap edge is approached and then decreases outside the air gap (Fig. 5). The force on the steel member is proportional to the square of this flux density gradient. Therefore, as the bias member rotates from the center of the air gap to the edge about the actuator pivot point, a nonlinear torque behavior is observed. Efforts can be made to alter the geometry and position of the member to achieve a more linear profile, but complex geometries increase cost and may not be possible due to spacial constraints. Shaping of the torque profile produced by the steel feature was achieved iteratively by changing the location and diameter of the steel member. The energy of the torque profile throughout the sweep angle was desired to be larger than the shock energy imparted to the drive. The torque profile was fit to an n-th order polynomial of the form

$$\phi(\theta) = \sum_{i=0}^{n} c_i \theta^i \tag{1}$$

where θ is the angular position and c_i is the i-th order coeffiecient. Noting that the magnetic bias opposes the arm torque when positive current is applied, the mechanical dynamics of the VCMA can be represented as

$$J\ddot{\theta} = K_t i - \phi(\theta) \tag{2}$$

where J is the arm inertia and K_t is the torque factor. The electrical circuit dynamics of the VCMA are described by

$$V_s = Ri + L\frac{di}{dt} + V_b \tag{3}$$

where R and L are the coil resistance and inductance, respectively, $V_b = K_t\dot{\theta}$ is the back electro-motive force, and V_s is the supply voltage which is the control signal. Choosing the states as $x_1 = \theta$, $x_2 = \dot{\theta}$, $x_3 = i$, and denoting the control input as $u = V_s$, the system can be represented in state-space form as

$$\dot{x} = Ax + Bu - B_\phi \phi(x_1), \tag{4}$$

$$A = \begin{bmatrix} 0 & 1 & 0 \\ 0 & 0 & \mu_0 \\ 0 & -\mu_2 & -\mu_3 \end{bmatrix}, \; B = \begin{bmatrix} 0 \\ 0 \\ \mu_4 \end{bmatrix}, \; B_\phi = \begin{bmatrix} 0 \\ \mu_1 \\ 0 \end{bmatrix}.$$

where $\mu_0 = K_t/J$, $\mu_1 = 1/J$, $\mu_2 = K_t/L$, $\mu_3 = R/L$, and $\mu_4 = 1/L$. It is noted that the matrix B_ϕ of the bias nonlinearity is not in the range space of the input matrix B. Therefore, the system does not satisfy the matching condition.

IV. CONTROLLER DESIGN

It was necessary to develop a control system capable of tracking predetermined trajectories generated from a reference model. In addition to tracking, the controller must be able to handle parameter variation. For the purpose of this study, it was assumed that the physical parameters of the motor were known and only the magnetic bias torque, specifically the polynomial coefficients, were uncertain. Although the exact value of the coefficients were unknown, the tolerances on the magnetic bias design were calculated and, therefore, the bias torque value within the actuator stroke angle could be bounded. To minimize vibration, acoustic energy, and power, it was desired that the reference model produce smooth trajectories for the controller to track. This was achieved by modeling the trajectory as a high-order polynomial with appropriate boundary conditions. Using the boundary conditions $\theta(0) = \dot{\theta}(0) = \ddot{\theta}(0) = \dddot{\theta}(0) = 0$, $\dot{\theta}(t_f) = \ddot{\theta}(t_f) = \dddot{\theta}(t_f) = 0$, and $\theta(t_f) = \theta_f$, the coefficients, β_i, of a unique seventh-order polynomial, $\theta_r(t) = \sum \beta_i t^i$, were determined ($i = 0, 1, \dots 7$). Trajectories were then defined for $\dot{\theta}_r$, $\ddot{\theta}_r$, and $\dddot{\theta}_r$. The reference trajectory for current was computed from

$$i_r(t) = (J/K_t)\ddot{\theta}_r(t) \tag{5}$$

and the reference voltage from

$$V_r(t) = (LJ/K_t)\dddot{\theta}_r(t) + Ri_r(t) + K_t\dot{\theta}_r(t). \tag{6}$$

Injecting the reference waveform (6) into the corresponding reference model

$$\dot{x}_r = Ax_r + BV_r \tag{7}$$

produces the state reference trajectory. The goal is to design a controller that will estimate the uncertain coefficients of the nonlinear bias in the dynamic model and result in trajectory tracking error convergence. Further, the nonlinear bias term $\phi(x_1)$ can be defined in the vector form as

$$\phi(x_1) = w^T c \tag{8}$$

where $w^T = [x_1^n, x_1^{n-1}, x_1^{n-2}, \cdots, 1]$ and $c^T = [c_n, c_{n-1}, c_{n-2}, \cdots, c_0]$. Let $e_j = x_j - x_{jr}$ be the error between the actual and reference trajectory of the j-th state. A Lyapunov function candidate is chosen as

$$V(s, \tilde{c}) = \frac{1}{2}(s_1^2 + s_2^2 + \tilde{c}^T\Gamma\tilde{c}) \tag{9}$$

where

$$s_1 = e_2 + \lambda e_1, \tag{10}$$

$$s_2 = \mu_0 e_3 + \mu_1 w^T\hat{c} + \alpha_1 e_1 + \alpha_2 e_2 \tag{11}$$

$\hat{c}$ is the estimate of the parameter vector c, $\tilde{c} = \hat{c} - c$, and λ, α_1, α_2 are user selected gains. The choice of s_1 was developed so that driving $s_1 \to 0$, also results in $e_1, e_2 \to 0$. The selection of s_2 is motivated by the fact that bias is not included in the reference model. Therefore, e_3 should take on some value that is proportional to the current required to offset the effects of magnetic bias. Hence, $s_2 \to 0 \implies \mu_0 e_3 \to -\mu_1 w^T\hat{c}$ in order to compensate for bias. Now consider the following control law [6]:

$$\begin{aligned} u = L[&\dot{x}_{3r} + \mu_2 x_{2r} + \mu_3 x_{3r} + \left(\rho_{11} + \rho_{12} w^T\Gamma^{-1}w\right) e_1 \\ &+ \left(\rho_{21} + \rho_{22} w^T\Gamma^{-1}w\right) e_2 + \left(\rho_{31} + \rho_{32} w^T\Gamma^{-1}w\right) e_3 \\ &+ \rho_{c1} x_2 v^T\hat{c} + \rho_{c2} w^T\hat{c} + \rho_{c3} w^T\Gamma^{-1}ww^T\hat{c}] \end{aligned} \tag{12}$$

where $v^T = [nx_1^{n-1}, (n-1)x_1^{n-2}, \cdots, 0]$, $\rho_{11} = -(\lambda + \alpha_1\alpha_3)/\mu_0$, $\rho_{12} = -\mu_1\sigma_1/\mu_0$, $\rho_{21} = (\mu_2\mu_0 - \alpha_1 - \alpha_2\alpha_3 - 1)/\mu_0$, $\rho_{22} = -\mu_1\sigma_2/\mu_0$, $\rho_{31} = \mu_3 - \alpha_2 - \alpha_3$, $\rho_{32} = -\mu_1\sigma_3/\mu_0$, $\rho_{c1} = -\mu_1/\mu_0$, $\rho_{c2} = \mu_1(\alpha_2 - \alpha_3)/\mu_0$, $\rho_{c3} = \mu_1^3\alpha_2/\mu_0$. As previously mentioned, bounds on the bias torque profile are known for a given drive population. This translates to bounds on the bias polynomial coefficients. With this knowledge, consider the function

$$\mathcal{P}(\hat{c}) = \hat{c}^T\hat{c} - c_u^\top c_u \tag{13}$$

where c_u is the known vector of coefficients that constitute the bias polynomial upper bound. A gradient projection algorithm [8] can be used to keep $\hat{c}$ within the convex set $\mathcal{S}$ where

$$\mathcal{S} := \{\hat{c} \in \mathbb{R}^n \,|\, \mathcal{P}(\hat{c}) \le 0\} \tag{14}$$

Now, consider the "smooth projection" $Proj$, which will be used to estimate $\hat{c}$ while maintaining (14). Let $\dot{\hat{c}} = Proj(\hat{c}, y)$ where

$$Proj(\hat{c}, y) = \begin{cases} y, \text{ if } \mathcal{P}(\hat{c}) < 0. \\ y, \text{ if } \mathcal{P}(\hat{c}) = 0 \text{ and } \nabla\mathcal{P}^\top y \le 0. \\ y - \Gamma\dfrac{\nabla\mathcal{P}^\top\nabla\mathcal{P}}{\nabla\mathcal{P}^\top\Gamma\nabla\mathcal{P}}y, \text{ otherwise,} \end{cases} \tag{15}$$

$$y = -\mu_1^2\alpha_2\Gamma^{-1}ww^T\hat{c} + (\sigma_1 e_1 + \sigma_2 e_2 + \sigma_3 e_3)\Gamma^{-1}w, \tag{16}$$

$\nabla\mathcal{P} = \left[\frac{\partial\mathcal{P}}{\partial\hat{c}}\right]^\top$, $\sigma_1 = -\mu_1(\lambda + \alpha_1\alpha_2)$, $\sigma_2 = -\mu_1(1 + \alpha_2^2)$, and $\sigma_3 = -\mu_1\alpha_2\mu_0$. Using the projection algorithm (15) along with the control law (12) results in

$$\dot{V} = -(\alpha_2 - \lambda)s_1^2 - \alpha_3 s_2^2 \le 0. \tag{17}$$

If the gains α_1, α_2 and λ are chosen such that $\alpha_2 > \lambda$, $-\alpha_1 + \alpha_2\lambda - \lambda^2 = 0$, and $\alpha_3 > 0$, $s_1 \in L_2 \cap L_\infty$, $s_2 \in L_2 \cap L_\infty$, and $\tilde{c} \in L_\infty$. Further, $\dot{s}_1 \in L_\infty$ and $\dot{s}_2 \in L_\infty$. Using Barbalat's lemma, $s_1 \to 0$ and $s_2 \to 0$. Since $s_1 = e_2 + \lambda e_1$, $e_1 \to 0$ and $e_2 \to 0$. Also, $s_2 \to 0 \implies \mu_0 e_3 \to -\mu_1 w^T\hat{c}$.

V. EXPERIMENTAL RESULTS

The physical parameters were measured for a single VCMA and used to generate the reference trajectories for a desired 5° seek angle. The following values of 48.26 g-cm^2, 71.5 N-mm/amp, 8.82 Ω, and 1.11 mH were measured for the inertia, torque factor, coil resistance, and coil inductance, respectively. The magnetic bias was also measured and is shown as a function of actuator sweep angle in Figure 6. Tolerance analysis showed that the bias could be bounded by a $\pm 7\%$ envelope about the nominal measurement. The bias was fit to polynomials of order three, four, and five. Performance comparisons were made using different estimates of the nonlinear bias function. Reducing the order of the polynomial estimate lowers the accuracy of the model and could increase the tracking error. However, the computation required for the control law is also reduced and, therefore, allows a sample rate increase and potentially improved tracking performance. The coefficients are given in Table I.

TABLE I

BIAS COEFFICIENTS

Order	c_5	c_4	c_3	c_2	c_1	c_0
3	-	-	0.0294	-0.0191	0.0002	0.0014
4	-	-0.2145	0.2802	-0.1133	0.0124	0.0011
5	0.4518	-0.8749	0.6232	-0.1883	0.0186	0.0098

Figure 7 depicts the experimental setup, which consisted of a drive containing the designed VCMA and a laser doppler vibrometer (LDV) to provide position and velocity feedback. The laser was targeted on the side of the actuator arm approximately 23.24 mm from the pivot. Because the discs are highly reflective, removing them was necessary to minimize the laser scatter and maintain a satisfactory measurement signal. Current feedback was achieved by measuring the voltage drop across a 0.2 Ω sense resistor.

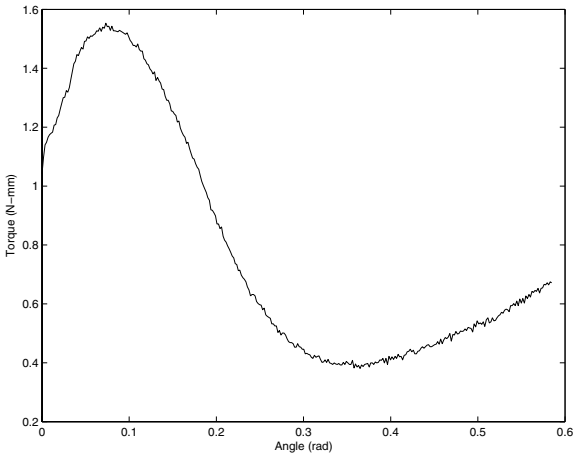

Fig. 6. Measured magnetic bias torque

Experiments were conducted to evaluate the controller design developed in the previous section. All tracking trajectories were designed for a 5° move. The control was chosen

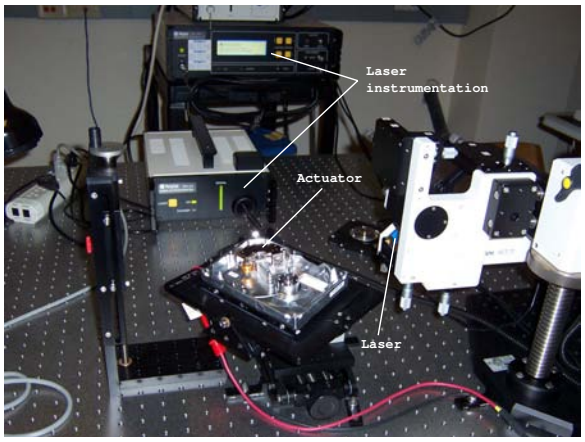

Fig. 7. Experimental setup

as (12) and the initial condition of the bias coefficient estimate was set at the upper bound $c_u^T c_u$. The sample rates were set at 30, 25, and 20 kHz for the bias estimate polynomials of 3, 4, and 5, respectively. Tuning showed the best trajectory tracking coefficients to be such that $\lambda = w_n$, $\alpha_1 = w_n^2$, $\alpha_2 = 2w_n$, and $\alpha_3 = w_n$ where $w_n = 400\pi$. The adaptation gains $\Gamma = \text{diag}\{\gamma_n, \cdots \gamma_0\}$ where n is the bias polynomial estimate order, were determined iteratively and are given in Table II. The estimated bias coefficients

TABLE II

ADAPTATION GAINS

Order	γ_5	γ_4	γ_3	γ_2	γ_1	γ_0
3	-	-	9.0e-11	8.0e-13	3.0e-13	3.0e-15
4	-	4.0e-9	8.0e-11	4.0e-13	9.0e-14	1.0e-15
5	1.0e-7	4.0e-9	1.0e-12	1.0e-13	1.0e-14	1.0e-15

for a 10 seek sample with $n = 5$ is shown in Figure 8. It was noted that the coefficients would occasionally drift outside the expected boundary limits during a given test run. To ensure that the coefficients remained close to the bounding limits, the gradient projection algorithm of (15) was implemented and included in the comparison. The results of the adaptive controller with projection for $n = 5$ are shown in Figure 9. Adaptive control with projection noticed a 12.4% and 1.6% increase in tracking error norm for position and velocity, respectively, when compared to adaptation without projection. The algorithm did effectively contain the coefficient trajectories and seemed to have the most influence on the higher order coefficients as shown in Figure 10. Projection was invoked 1262 times in a 2000 point, 10 seek sample run. Reducing the order of the polynomial fit decreases the performance of the controller as expected. However, some or all of the performance could be recovered with a sample rate increase. In fact, a fourth order bias polynomial estimate outperformed the fifth-order estimate when the sample rate was increased by 5 kHz. The third-order estimate came close to achieving that of the fifth-order with a 10 kHz increase. Therefore, if the sampling resources are available, the complexity of the controller can

be reduced while maintaining comparable performance. The comparison results are summarized in Table III.

TABLE III

CONTROLLER PERFORMANCE ERROR L_2 NORM.

Rate→	20 kHz		25 kHz		30 kHz	
Order↓	e_1	e_2	e_1	e_2	e_1	e_2
3	0.0517	17.11	0.0313	14.77	0.0182	11.21
4	0.0329	13.92	0.0153	10.34	-	-
5	0.0161	11.94	-	-	-	-

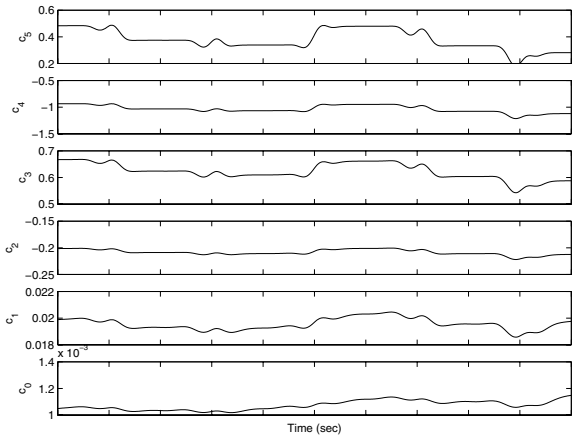

Fig. 8. Estimated coefficient dynamics without projection

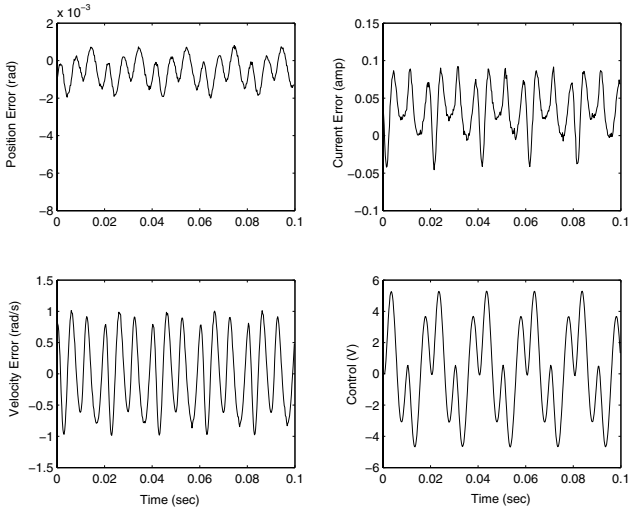

Fig. 9. Controller performance with projection (10 seek sample, $n = 5$)

VI. CONCLUSION

A non-contact, magnetic bias latching mechanism was designed to fulfill the rotary, non-operational shock requirements of a disc drive. The resulting behavior of the bias torque profile was nonlinear throughout the actuator sweep angle. A third-order dynamic model was developed for the VCMA, which included the bias force nonlinearity.

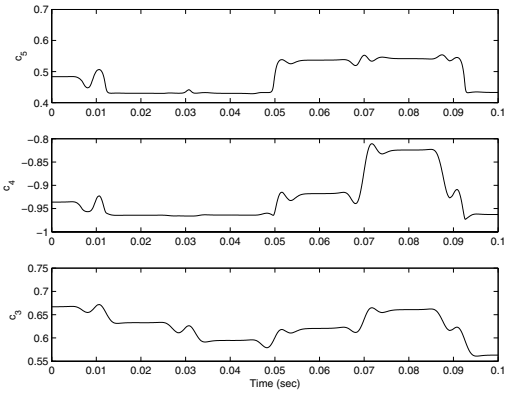

Fig. 10. High order coefficient dynamics with projection

Measurements were taken of the magnetic bias torque and the motor physical parameters. It was assumed that the bias measurement was nominal and bounds were determined based on geometric tolerance analysis to represent a production population. An adaptive controller was developed to track predetermined reference trajectories and compensate for the bias uncertainty. Since bounds on the bias estimate were known, a projection algorithm was implemented to constrain the bias estimate within the known bounds. Experiments were conducted comparing the adaptive control with and without projection. Adding projection resulted in slightly reduced performance. Performance effects from variation in bias estimate accuracy and sample rate were also investigated. It was determined that controller performance lost by a reduction in bias modeling accuracy could be recovered by an increase in sample rate. Therefore, if sampling resources are available, the complexity of the controller can be reduced without significant sacrifices in performance. Velocity feedback was available for the experiments of this study. Considering that production disc drives do not have direct velocity feedback, future work will focus on the output feedback case with an observer.

REFERENCES

[1] S. G. Campbell, "Magnetically biased aerodynamically released integral safety latch for rigid disk drive", U.S. Patent 4692829, Sep. 8 1987.

[2] J. H. Morehouse, J. A. Dunckley, D. M. Furay, "Rotary inertial latch for disk drive actuator", U.S. Patent 5189576, Feb. 23, 1993.

[3] G. Kelsic, J. Martinez, "Magnetic latch for disk drive actuator", U.S. Patent 5023736, Jun. 11 1991.

[4] R. C. Reinhart, "Disk drive magnetic actuator latch mechanism having a latch lever with magnetic members on each end thereof for latching and unlatching the actuator using voice coil motor magnet", U.S. Patent 5734527, Mar. 31 1998.

[5] Y. Kinoshita et al., "Actuator arm with magnetic flux response to bias arm to a stop position", U.S. Patent 5541792, Jul. 30 1996.

[6] R. T. Ratliff, P. R. Pagilla, "Design and Seek Control of a Disc Drive Actuator with Nonlinear Magnetic Bias", *Proc. IEEE Int. Conf. Robotics and Automation*, New Orleans, LA, pp. 3640–3646, Apr. 2004.

[7] H. K. Khalil, *Nonlinear Systems*, 3rd ed. Prentice Hall, NJ, 2002.

[8] P. A. Ioannou, J. Sun, *Robust Adaptive Control*, Prentice-Hall, NJ, 1996.